Bistability in droplet traffic at asymmetric microfluidic junctions

Pravien Parthiban[1] and Saif A. Khan[1,2,a)]
[1]*Singapore-MIT Alliance, National University of Singapore, 4 Engineering Drive 3, E4-04-10, Singapore 117576*
[2]*Department of Chemical and Biomolecular Engineering, National University of Singapore, 4 Engineering Drive 4, E5-02-28, Singapore 117576*

(Received 8 May 2013; accepted 13 August 2013; published online 23 August 2013)

We present the first experimental demonstration of confined microfluidic droplets acting as discrete *negative* resistors, wherein the effective hydrodynamic resistance to flow in a microchannel is *reduced* by the presence of a droplet. The implications of this hitherto unexplored regime in the traffic of droplets in microfluidic networks are highlighted by demonstrating bistable filtering into *either* arm of symmetric and asymmetric microfluidic loops, and programming oscillatory droplet routing therein. © *2013 AIP Publishing LLC*. [http://dx.doi.org/10.1063/1.4819276]

I. INTRODUCTION

Droplet microfluidics involves the ordered formation and transport of immiscible liquids as droplets in engineered microchannels. Driven by a number a unique advantages caused by microscale confinement, droplet microfluidics has elicited significant research interest over the past decade, and has shown much promise in chemical and biological analytics, colloidal and chemical synthesis, and drug discovery.[1–6] Integration of multiple functionalities in a single platform and increasing device throughputs through parallelization often result in devices with a highly complicated network of microchannels.[7–9] Engineering droplet flows in such devices is challenging; the traffic of a train of identical droplets through the most rudimentary microchannel network consisting of a single bifurcation or loop can exhibit complex behavior characteristic of non-linear dynamical systems.[10–15] Therefore, the ability to understand, predict, and control the traffic of droplet ensembles in microchannel networks is invaluable to the design and robust operation of multiplexed, multifunctional droplet microfluidic devices.

A droplet train can be viewed as a flow of discrete resistors where each droplet modifies the effective hydrodynamic resistance to flow of a microchannel.[10–18] The complex non-linear dynamics of droplet traffic in microchannel networks is primarily due to this discrete nature of the flow. Each droplet that arrives at a microfluidic junction, if it does not break up or interact with adjacent droplets, gets routed into the arm which has, at that instant, a higher rate of flow into it.[10–18] Thus, droplet routing at microfluidic junctions is governed by hydrodynamic resistances of downstream channels, which in turn vary dynamically with the entry and exit of each droplet. Such hydrodynamic feedback implies that the path taken by a given droplet through a microfluidic network is inextricably linked to the paths traversed by the previous ones, thus, the traffic of droplet ensembles in microchannel networks can exhibit highly complex dynamics. Crucial to elucidating such dynamics is the precise quantification of how droplets modify the effective hydrodynamic resistance of a microchannel. Furthermore, an ability to predict the hydrodynamic resistance of droplet filled microchannels is essential to engineer facile strategies to regulate droplet traffic in microfluidic networks, be it using active methods that rely on external actuation,[19–23] or passive ones that rely purely on elegantly designed microfluidic circuitry.[16,24–27]

[a)]Electronic mail: chesakk@nus.edu.sg

Thus far, all experimental investigations and theoretical treatments of droplet traffic in microfluidic networks have exclusively focused on the case where droplets *increase* the effective hydrodynamic resistance of the microchannel, acting therefore as discrete positive resistors.[10–18] While regimes where the inner phase lowers the resistance to flow have been previously accessed in gas-liquid systems,[28,29] such regimes have not been explored yet in liquid-liquid droplet microfluidic flows. In fact, the most widely used models to describe droplet traffic explicitly assume the effective resistance added by droplets to be a constant, independent of droplet size and speed.[11–13,30] In contrast, in this paper, we show that low viscosity confined microfluidic droplets, above a threshold speed of propagation dependent solely on their length, start acting as discrete *negative* resistors, wherein droplets *decrease* the effective hydrodynamic resistance of the microchannel. Furthermore, we highlight an important consequence of this hitherto unexplored regime by showing that an incoming droplet train can sort entirely and exclusively into *either* arm of both symmetric and asymmetric microfluidic junctions. Such bistable filtering is both interesting and previously unforeseen; with droplets acting as discrete positive resistors the only possible filtering is into the shorter arm of an asymmetric junction.[17,18] Additionally, we exploit the existence of bistable filtering to regulate droplet traffic at microfluidic junctions.

II. RESULTS AND DISCUSSION

In our experiments, we worked with an immiscible liquid-liquid system consisting of an ionic liquid as the continuous phase (viscosity $\mu = 0.022\,\text{Pa.s}$) and water as the dispersed phase (viscosity $\lambda\mu = 0.001\,\text{Pa.s}$). The ionic liquid, 1-ethyl-3-methyl-immidazolium bis(trifluoromethylsulfonyl)imide ([EMIm][NTf2]), was specifically chosen because it spontaneously spread on the microchannel surface fabricated out of poly(dimethylsiloxane) (PDMS) in the presence of water and was able to form ordered droplets of water in the absence of surfactants. The interfacial tension between the liquids was $\sigma \sim 0.01\,\text{N/m}$. The ionic liquid used dissolves a finite amount of water (approximately two weight percent at ambient conditions), thus, prior to it being used in experiments, the ionic liquid was saturated with water.

A. Hydrodynamic resistance of a microchannel filled with droplets

We first experimentally measured the hydrodynamic resistance (R^n) of a microchannel filled with n water droplets of length l_D, separated by ionic liquid slugs of length l_S, and translating with a speed U. The pressure drop across the microchannel ΔP was directly measured, and subsequently R^n was calculated as $\Delta P/Q$, where Q is the total rate of flow through the microchannel.

ΔP is typically modeled as the sum of pressure drops across all the droplets and continuous phase liquid slugs,[17,18,31,32] thus, R^n can be written as

$$R^n = R^0[1-\phi] + nR_D, \tag{1}$$

where R^0 is the hydrodynamic resistance of the microchannel completely filled with the continuous phase. For channels of rectangular cross-section where $h < w$, R^0 is given by[33]

$$R^0 = \frac{12\,\mu L}{[h^3 w(1-0.63h/w)]} = \alpha L, \tag{2}$$

$\phi = nl_D/L$ is the fraction of the microchannel occupied by droplets and R_D is the resistance to flow of a single droplet moving with a speed U. The hydrodynamic resistance of the portion of the microchannel without droplets, $R^0[1-\phi]$, is approximated here with the assumption that flow is fully developed across the lengths of all the continuous phase liquid slugs, a reasonable assumption at low Reynolds numbers ($Re = hU\rho/\mu$, where ρ is the density of the continuous phase), such as those accessed in our experiments ($Re < 1$).[17,18,32] Another implicit assumption in the model for R^n is that the relative speed between the droplet and the surrounding

continuous phase is negligible; we find that our measurements of U are within 10% of Q/A, thus, confirming the validity of this assumption.[34]

It is illustrative to recast the expression for R^n as

$$R^n = R^0 - n\alpha l_D\left[1 - \frac{R_D}{\alpha l_D}\right]. \tag{3}$$

Here, αl_D is the hydrodynamic resistance of a microchannel of length equal to the droplet length filled completely with the continuous phase, or in other words, the resistance to flow originally contributed by the segment of continuous phase liquid displaced by the presence of the droplet. From the above expression, it is evident that the effective change in the hydrodynamic resistance of microchannel caused by the presence of a single droplet is given by $-\alpha l_D[1 - R_D/(\alpha l_D)]$ or $R_D - \alpha l_D$. The relative magnitudes of R_D and αl_D determine if droplets increase or decrease the resistance to flow. It can be clearly seen that droplets will act as negative resistors and reduce the hydrodynamic resistance of a microchannel when $R_D/(\alpha l_D) < 1$.

R_D in turn can be written as $R_D = \Delta P_D/(Uwh)$, where ΔP_D is the pressure drop across a droplet moving with a speed U. ΔP_D typically has two contributions, one due to the capillary pressure jumps across the liquid-liquid interfaces at the droplet front and rear, and the other due to the viscous dissipation along the length of the droplet.[31,35] The latter scales as $\lambda\mu U l_D/h^2$;[31,35] whilst the former depends on flow induced perturbation of the liquid-liquid interfaces at the droplet front and rear. The shapes of the front and rear end caps of the droplet are identical when the droplet is at rest. In cases where the continuous liquid completely wets the channel wall, once the droplet is set in motion, a film of the continuous phase liquid is deposited around the droplet. Film deposition at the front of the droplet and drainage at the rear of the droplet perturb the shapes of front and rear end caps of the droplet differently. This causes a net difference in the capillary pressure jumps across the liquid-liquid interfaces at the droplet front and rear. This difference in the capillary pressure jumps depends on the thickness of the continuous phase liquid film encapsulating the droplet, and at low capillary numbers scales as $\sim(2\sigma/h)Ca^{2/3}$, where $Ca = \mu U/\sigma$ is the Capillary number.[31,35–37] Thus,

$$\Delta P_D \sim \left(\frac{2\sigma}{h}\right)Ca^{2/3}\left[1 + \lambda\frac{Ca^{1/3}l_D}{h}\right], \tag{4}$$

when $\lambda Ca^{1/3}l_D/h \ll 1$, the viscous contributions can be ignored and

$$\Delta P_D \sim \left(\frac{2\sigma}{h}\right)Ca^{2/3}. \tag{5}$$

In gas-liquid microfluidic segmented flows, where the gas phase viscosity can be readily neglected ($\lambda \ll 1$), models similar to that given in Eq. (5) have been used to successfully quantify the pressure drops across bubbles translating through both circular capillaries[38] and rectangular microchannels.[29] Furthermore, in liquid-liquid systems, models similar to that given in Eq. (4) have accurately predicted the experimentally measured pressure drops across confined droplets translating through circular capillaries.[35] Thus far though, experiments with droplet transport in rectangular capillaries at high capillary numbers have been inconclusive.[39,40]

We first check the validity of the model for ΔP_D in droplet transport through rectangular microchannels, specifically in the case where the viscous contributions in the droplet can be ignored. In our experiments, $\lambda \sim 0.05$, $Ca \in [10^{-4} - 10^{-2}]$ and $l_D/h \in [3 - 8]$, therefore, $\lambda Ca^{1/3}l_D/h$ is always $\ll 1$. Furthermore, when $\lambda \ll 1$, as is the case here, droplets essentially behave like an inviscid bubbles and the thickness of the deposited film in droplet transport will not be affected by droplet viscosity, and thus, the magnitude of the capillary contributions to ΔP_D should be identical to that of an inviscid bubble.[41] From our experimental measurements of ΔP, we calculate ΔP_D,

$$\Delta P_D = \frac{\Delta P}{n} - \frac{12\mu U l_S}{h^2[1 - 0.63h/w]}. \tag{6}$$

Our experiments show that

$$\Delta P_D = 4.36\left(\frac{2\sigma}{h}\right)Ca^{2/3} \tag{7}$$

and is independent of droplet length [Fig. 1(c) inset]—this compares favorably to the theoretical prediction of Wong *et al.* for bubble transport in a microchannel of rectangular cross-section with $w/h = 2$.[37]

Now, with $R_D = 4.36(2\sigma/h)Ca^{2/3}/(Uwh)$, the hydrodynamic resistance of a rectangular microchannel filled with n droplets can finally be written as

$$R^n = R^0 - n\alpha l_D\left(1 - 0.54\frac{h}{l_D Ca^{1/3}}\right). \tag{8}$$

The above equation can further be simplified by noting that $R^0 = \alpha L$

$$R^n = \alpha\left[L - nl_D\left(1 - 0.54\frac{h}{l_D Ca^{1/3}}\right)\right]. \tag{9}$$

Crucially, it can be seen that the experimentally measured $R_D < \alpha l_D$ when $0.54hl_D^{-1}Ca^{-1/3} < 1$ [Fig. 1(c)]. Droplets thus act as negative resistors above a threshold capillary number

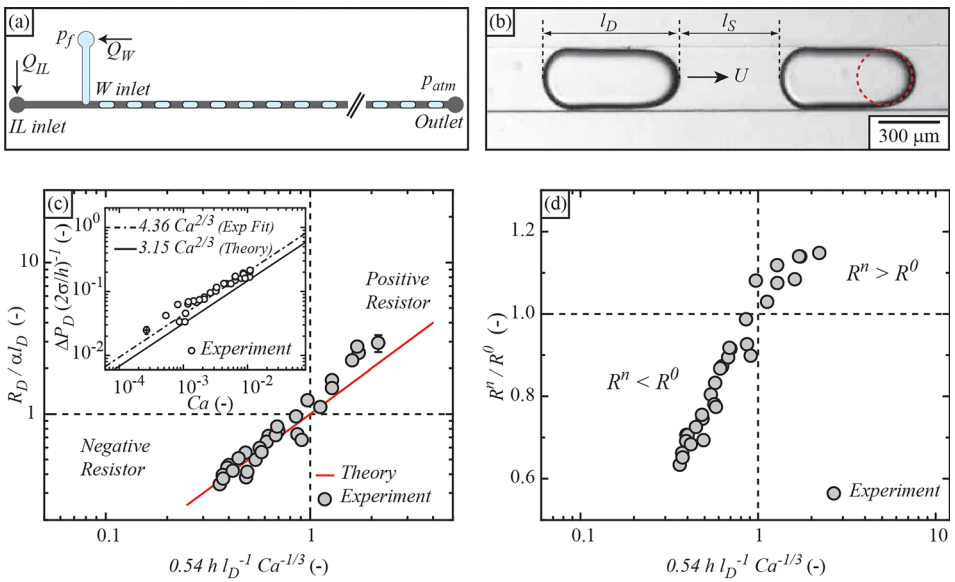

FIG. 1. (a) Sketch of the experimental setup for measurement of the effective hydrodynamic resistance to flow of a microchannel filled with n droplets, R^n. (b) Micrograph of water droplet flow in a microchannel filled with the ionic liquid, absence of contact lines indicates that the water droplets are completely encapsulated with an ionic liquid film. (c) Inset: The pressure drop across confined droplets in rectangular microchannels agrees reasonably well with the theory for inviscid bubbles. Here, $l_D/h \in [3-8]$ and $l_S/h \in [5-50]$. (c) Comparison of the magnitudes of R_D and αl_D. The effective change in the hydrodynamic resistance of microchannel caused by the presence of a single droplet is given by $R_D - \alpha l_D$. Experimentally measured R_D is less than αl_D and droplets therefore should act as discrete negative resistors when $0.54hl_D^{-1}Ca^{-1/3} < 1$. (d) It is indeed seen that when $0.54hl_D^{-1}Ca^{-1/3} < 1$ the experimentally measured hydrodynamic resistance of a microchannel filled with n droplets, R^n is less than that of a microchannel devoid of droplets, R^0.

$$Ca_T = \left(0.54\frac{h}{l_D}\right)^3. \tag{10}$$

When droplets act as negative resistors the hydrodynamic resistance of a microchannel filled with droplets should be less than that of a microchannel devoid of droplets and filled entirely with the continuous phase liquid. Our experimental measurements illustrate that indeed $R^n < R^0$ when $Ca > Ca_T$ [Fig. 1(d)].

B. Bistable filtering of droplets at a microfluidic junction

We now demonstrate an interesting and unexpected implication of confined microfluidic droplets acting as discrete negative resistors during their traffic through microchannel networks. Each droplet that arrives at the inlet of a microfluidic junction, if it does not break up or interact with adjacent droplets, will get directed into the arm that has the highest flow rate at that instant.[10–18] When droplets act as positive resistors an incoming train can only filter into the shorter arm of an asymmetric microfluidic loop.[17,18] Therein, with droplets increasing the resistance to flow, the filter regime is accessed if the number of droplets in the shorter arm is below a threshold; the shorter arm then has a lower hydrodynamic resistance and consequently a higher rate of flow into it. This is achieved when the incoming droplet train has a high dilution (large inter-droplet distance). Decreasing the dilution of the incoming train increases the number of droplets in the shorter arm and consequently increases its hydrodynamic resistance. At a certain low dilution, the hydrodynamic resistance of the droplet filed shorter matches that of the empty longer arm and any further decrease in the dilution of the incoming train results in the droplets being distributed between both the arms of the junction.

In contrast, when droplets act as discrete negative reactors they can stably filter into either arm of symmetric and asymmetric loops. As incoming droplets get directed into the arm with the higher rate of flow into it, or conversely, a lower hydrodynamic resistance, a droplet train will filter at a microfluidic loop if $R_i^{n_i}$, the hydrodynamic resistance of arm i filled with n_i droplets moving with a speed U_i, is lesser than that of the other arm completely devoid of droplets.

A train of monodisperse droplets of length l_D, inter-droplet distance l_S, and speed of propagation U_0 will filter into one of the arms, say arm 1, of a symmetric microfluidic loop (with arms of identical lengths $L_1 = L_2$), if $R_1^{n1} < R_2^0$. From Eq. (9), we have the condition for filtering into arm 1 of a symmetric junction

$$L - n_1 l_D\left(1 - 0.54\frac{h}{l_D Ca_1^{1/3}}\right) < L. \tag{11}$$

From the above equation, it is clear that the droplet train will filter into arm 1 if $0.54 h l_D^{-1} Ca_1^{-1/3} < 1$, or $Ca_1 > Ca_T$, in other words, when droplets act as negative resistors as they translate through arm 1 of the symmetric junction. It can be further seen that $Ca_1 > Ca_T$ the incoming train will filter into arm 1 irrespective of the number of droplets in arm 1. Indeed, if the very first droplet of the incoming train enters arm 1 of the otherwise empty microfluidic loop (filled only with the continuous phase) with a speed $U_1 = 0.5U_0$ high enough such that it acts as a negative resistor, the entire train will filter into arm 1; each successive droplet that enters arm 1 will contribute to a further decrease in the resistance of arm 1, thus, at steady state, $R_1^{n_1} < R_2^0$. When the incoming train is filtering into arm 1, the speed of propagation of the droplets through arm 1, $U_1 > 0.5U_0$, therefore, the critical capillary number of the incoming train required for accessing the filter regime in symmetric junctions is given by $Ca_{sym} = 2Ca_T$. We have previously shown such transitions with confined microfluidic bubbles.[29]

Interestingly, in *asymmetric* microfluidic loops with arms of unequal lengths ($L_2 = \delta L_1$, where $\delta > 1$), the incoming train will filter into the *longer* arm if the droplet filled longer arm has a lower hydrodynamic resistance, $R_2^{n_2} < R_1^0$. Again from Eq. (9), we have the condition for filtering into the longer arm of an asymmetric junction

$$\delta L_1 - n_2 l_D \left(1 - 0.54 \frac{h}{l_D Ca_2^{1/3}}\right) < L_1. \tag{12}$$

From the above equation, it is clear that for the droplet train to filter into the longer arm not only should the droplets act as negative resistors as they translate through longer arm, $0.54 h l_D^{-1} Ca_2^{-1/3} < 1$, or $Ca_2 > Ca_T$, but also at steady state the number of droplets in longer arm, n_2, should be greater than a threshold. When the incoming train filters into the longer arm, the flow rate into it is larger, thus, $U_2 > 0.5U_0$. Additionally, the number of droplets in the longer arm can be calculated as $n_2 = (L_2/U_2)f$, where f is the frequency with which the droplets flow into the asymmetric microfluidic loop. From the above analysis, one can readily determine critical capillary number of the incoming train required for filtering into the longer arm of an asymmetric junction[34]

$$Ca_{asym} = \left(\frac{1}{1-\zeta}\right)^3 Ca_{sym}, \tag{13}$$

where $\zeta = 0.5(\delta - 1)\delta^{-1}\phi^{-1}$ can be viewed as a morphological parameter dependent on the asymmetry of the junction and the spatial periodicity of the incoming droplet train. It can be seen that Ca_{asym} diverges as ζ approaches 1 [Fig. 2(c)]. This illustrates the fact that for a given junction asymmetry, incoming trains having a void fraction ϕ less than $0.5(\delta - 1)/\delta$ cannot filter into the longer arm, herein, n_2 can never be high enough such that $R_2^{n_2} < R_1^0$.

We carried out rigorous experiments with both symmetric ($L_1 = L_2 = 10.3$ cm) and asymmetric ($L_1 = 10.3$ cm, $L_2 = \delta L_1$, $\delta = 1.1,\ 1.2$) microfluidic loops to account for transition into filter regimes.[34] In symmetric junctions, filtering could be readily be achieved by ensuring droplets behave as negative resistors. In asymmetric junctions, when droplets act as negative resistors, the incoming train always filters, by default, into the shorter arm as it has a lower resistance. To test if stable filtering into the longer arm can occur, we initially force the train to filter into the longer arm by injecting a stream of ionic liquid to the shorter arm, this external forcing is subsequently stopped to see if the train continues to filter into the longer arm. We find that our experimental observations of filtering are inline with our theoretical predictions. Filter regime in symmetric junctions is accessed by increasing the speed of propagation of the incoming train; whilst filtering into the longer arm of an asymmetric microfluidic loop is also accessed by reducing the dilution of the incoming train to increase the number of droplets in the longer arm.[34] Importantly, our experimental measurements of Ca_{sym} and Ca_{asym} agree reasonably well with our theoretical predictions [Fig. 2(c)].

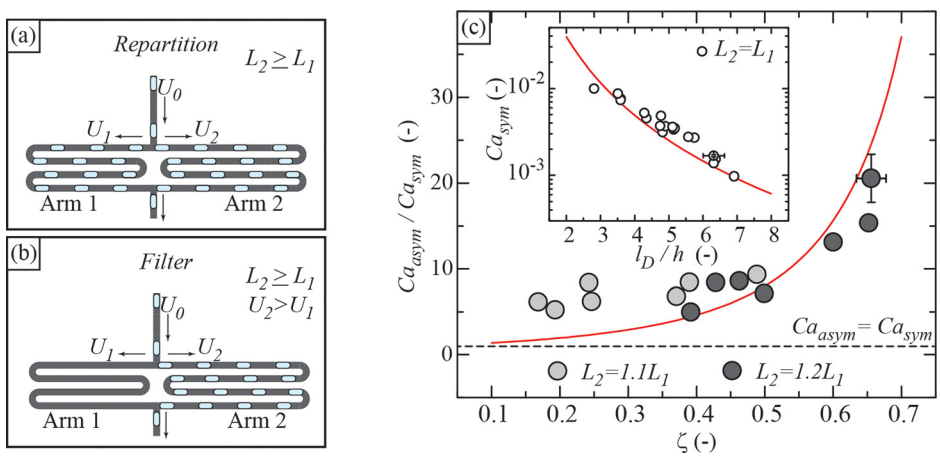

FIG. 2. Schematic of repartition (a) and filter (b) regimes during droplet traffic through microfluidic loops. (c) Experimental measurements (symbols) of threshold capillary numbers for filtering droplets into the longer arm of a asymmetric loop, Ca_{asym} and in symmetric loops, Ca_{sym} (inset) agree reasonably well with the theory (solid lines).

C. Droplet traffic control

The most important consequence of our analysis is the existence of *bistability* in droplet routing, where the train can be entirely and stably routed into *either* arm of an asymmetric loop. We exploit the existence of this bistability to program oscillatory routing of droplet trains in microfluidic loops by switching between the two stable flow states. Switching is achieved with the aid of a *switching flow*—a stream of continuous phase injected into arm i of the loop the incoming train is filtering into. Increasing the switching flow rate Q_{Ci} decreases the rate of flow into arm i.[42] The rate of flow into arm i becomes less than that into the other arm above a threshold Q_{Ci}, and the incoming droplets get forcibly routed into the other arm. As filtering into both arms are stable only a finite pulse of the switching flow needs to be injected. Thus, with the incoming train filtering into one of the arms of the microfluidic loop, an external trigger in form of a pulsed injection of the continuous phase of sufficient flow rate and duration into the said arm is used to stably switch the filtering of the incoming train into the other arm. The minimum duration of this pulse, τ_P, required to switch the filtering from say arm 1 to arm 2, can be estimated as $\tau_P \sim L_2/0.5U_0$, the approximate time required to fill the entire length of arm 2 with droplets. In our experiments, we used a switching flow rate Q_C of at least half the total flow rate into the loop to achieve switching. We readily generated oscillatory bistable flows of varying periods at the microfluidic loop with programmed injection of pulses of the continuous phase ($\tau_P = 10$ s) into both arms of a microfluidic loop. We were able to flexibly tune the periods of oscillation from 120 s to 20 s [Fig. 3].

In our experiments, we have focused on a system where the droplet viscosity is far less than that of the continuous phase, $\lambda \ll 1$. It would be interesting to know if droplets can act as negative resistors at higher values of λ where the viscous dissipation across the length of the droplet cannot be ignored. In their recent work, Vanapalli and co-workers directly measured using a microfluidic comparator, the excess pressure drop across a microchannel through which a single droplet is convected; they find that the excess pressure drop decreases when λ is increased from 0.03 to 0.88.[40] This indicates that with a moderate increase in λ it might indeed be easier to access regimes where droplets act as negative resistors. Additionally, we in our experiments explore a liquid-liquid immiscible system devoid of surfactants. The presence of surfactants or trace impurities can cause ΔP_D to increase by a factor of $4^{2/3}$ due to Marangoni

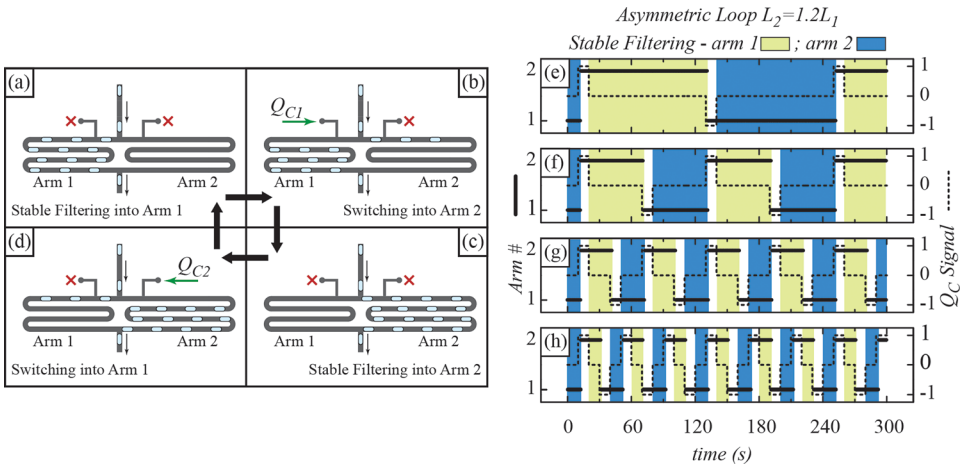

FIG. 3. (a)–(d) Illustration of oscillatory droplet routing at a microfluidic junction; with the incoming droplet train filtering into arm i of the loop, a finite pulse of the continuous phase is injected into arm i to switch the filtering into the other arm. (enhanced online) [URL: http://dx.doi.org/10.1063/1.4819276.1] [URL: http://dx.doi.org/10.1063/1.4819276.2] [URL: http://dx.doi.org/10.1063/1.4819276.3] [URL: http://dx.doi.org/10.1063/1.4819276.4]. (e)–(h) Plots tracking the trajectories of the droplet train at an asymmetric microfluidic loop, $L_2 = 1.2L_1$ showing oscillatory routing; the arm into which the train is filtering into is plotted as solid black lines. The time dependent injection of the continuous phase to effect switching is represented by $Q_{C_{signal}}$, which is plotted as dashed black lines. $Q_{C_{signal}} = 1$ and -1 when the continuous phase at a flow rate of 20μl/min is injected exclusively into arms 1 and 2, respectively, and $Q_{C_{signal}} = 0$ when there is no injection into either arm.

stresses at the droplet boundary.[43] This should result in the threshold capillary number beyond which droplets function as negative resistors to increase by a factor of 4^2. With the use of higher viscosity continuous phase liquids, such high capillary numbers should still be readily accessible.

III. CONCLUSIONS

In conclusion, we have described a hitherto unexplored regime in microfluidic droplet transport where the effective hydrodynamic resistance to flow of a microchannel decreases with an increase in the number of droplets present. Droplets acting as discrete negative resistors can exhibit exciting and counterintuitive dynamical response in microfluidic networks, and can also enable facile control of traffic in such networks. The findings presented here should serve to further the understanding of the dynamics of droplets ensembles in both man made microchannel networks and natural ones such those that occur in porous media and respiratory airways. Additionally, we have also shown the use of an ionic liquid as the continuous phase; ionic liquids, essentially molten salts, have garnered significant attention recently due to their unique physical and chemical properties which can be readily tuned.[44] The use of chemically functional continuous phase along with the ability to regulate droplet traffic in microfluidic network should aid in extending the reach of droplet microfluidics into yet uncharted territories.

IV. EXPERIMENTAL METHODS

A. Device fabrication

We performed our experiments with microfluidic devices made of PDMS. Standard photolithography techniques were used to fabricate SU8-on-Silicon masters. These masters were subsequently used to mold PDMS replicas; in brief a 10:1 weight ratio of PDMS base and curing agent (Sylgard 180 kit, Dow Corning) was mixed thoroughly and degassed, the mixture was subsequently poured over the master and cured for approximately 2 h at 70 °C. After carefully peeling off the master, the PDMS replica was thoroughly cleaned using scotch tape and holes for the inlets and outlets were punched. Air plasma treatment was used to bond the PDMS replica to a flat slab of PDMS molded from a plain Silicon wafer (the flat slab of PDMS was bonded to a plain glass slide prior to this step). After the bonding and glueing of the inlet and outlet tubes, the microchannel was placed in an oven set at 100 °C for at least 24 h before being used. This empirical protocol yielded a highly hydrophobic microchannel that did not wet water, the dispersed phase used in the droplet traffic experiments.

B. Droplet microfluidic experiments

In the experiments to measure the hydrodynamic resistance (R^n) of a microchannel filled with droplets, we used microchannels with length $L = 0.683$ or 1.66 m, and rectangular cross section (width $w = 300\,\mu$m and height $h = 123\,\mu$m). Water droplets of length l_D, separated by ionic liquid slugs of length l_S, and translating with a speed U were generated at a standard T-junction droplet generator by pumping in the ionic liquid and water at flow rates q_{IL} and q_W, respectively, using syringe pumps. l_D and U were varied systematically by varying q_{IL} and q_W. The schematic of experimental setup is given in Fig. 1(a). A pressure transducer attached to the water inlet was used to measure pressure drop across the microchannel ΔP, and subsequently R^n was calculated as $\Delta P/Q$, where Q is the total rate of flow through the microchannel given by $Q = q_{IL} + q_W$.

Experiments to study droplet traffic at symmetric and asymmetric junctions were carried out in microfluidic devices comprising of a microfluidic loop located downstream of a standard T-junction droplet generator. The microchannels had a rectangular cross section (width $w = 300\,\mu$m and height $h = 123\,\mu$m). Three different microfluidic loop geometries were studied, one symmetric ($L_1 = L_2 = 10.3$ cm) and two asymmetric ($L_1 = 10.3$ cm, $L_2 = \delta L_1$, $\delta = 1.1$, 1.2). Ionic liquid and water were pumped into the droplet generator using syringe pumps (PHD 2000, Harvard Apparatus) at flow rates of q_{L1} and q_W, respectively, to form mono disperse

droplets of water of length l_D separated by ionic liquid segments of length l_S propagating at a speed U. l_B, l_S, and U were all controlled by varying q_W and q_{L1}. An additional feed inlet located downstream of the T-junction droplet generator pumped in ionic liquid at a flow rate q_{L2} so as to provide greater flexibility in varying both l_S and U. In experiments where the filtering of the incoming droplet train needed to be switched between two arms of the microfluidic loop, the devices used had two further inlets to pump in ionic liquid into each arm of the loop to effect switching.[34]

The details of the flow were captured using a video camera (Basler pi640) mounted on a stereo microscope (Leica MZ 16). The parameters of the droplet train generated (l_D, l_S, and U) were measured and trajectories of individual droplets at the microfluidic loop were analyzed using image processing algorithms implemented in MATLAB to analyze video micrographs of the flow.

ACKNOWLEDGMENTS

P.P. and S.A.K. acknowledge funding from the CPE program of the Singapore-MIT Alliance. The authors thank Dr. R. Akkipedi from the ASTAR Institute of Materials Research and Engineering for providing access to lithography facilities and are greatly indebted to Professor Michiel T. Kreutzer for invaluable discussions.

[1]A. Gunther and K. F. Jensen, Lab Chip **6**, 1487 (2006).
[2]H. Song, D. L. Chen, and R. F. Ismagilov, Angew. Chem., Int. Ed. **45**, 7336 (2006).
[3]A. Huebner, S. Sharma, M. Srisa-Art, F. Hollfelder, J. B. Edel, and A. J. deMello, Lab Chip **8**, 1244 (2008).
[4]S.-Y. Teh, R. Lin, L.-H. Hung, and A. P. Lee, Lab Chip **8**, 198 (2008).
[5]J.-T. Wang, J. Wang, and J.-J. Han, Small **7**, 1728 (2011).
[6]M. T. Guo, A. Rotem, J. A. Heyman, and D. A. Weitz, Lab Chip **12**, 2146 (2012).
[7]N. de Mas, A. Gunther, T. Kraus, M. Schmidt, and K. Jensen, Ind. Eng. Chem. Res. **44**, 8997 (2005).
[8]J. Shim, G. Cristobal, D. R. Link, T. Thorsen, Y. Jia, K. Piattelli, and S. Fraden, J. Am. Chem. Soc. **129**, 8825 (2007).
[9]H. R. Sahoo, J. G. Kralj, and K. F. Jensen, Angew. Chem., Int. Ed. **46**, 5704 (2007).
[10]M. J. Fuerstman, P. Garstecki, and G. M. Whitesides, Science **315**, 828 (2007).
[11]F. Jousse, R. Farr, D. R. Link, M. J. Fuerstman, and P. Garstecki, Phys. Rev. E **74**, 036311 (2006).
[12]O. Cybulski and P. Garstecki, Lab Chip **10**, 484 (2010).
[13]T. Glawdel, C. Elbuken, and C. Ren, Lab Chip **11**, 3774 (2011).
[14]V. Labrot, M. Schindler, P. Guillot, A. Collin, and M. Joanicot, Biomicrofluidics **3**, 012804 (2009).
[15]D. A. Sessoms, A. Amon, L. Courbin, and P. Panizza, Phys. Rev. Lett. **105**, 154501 (2010).
[16]G. Cristobal, J. P. Benoit, M. Joanicot, and A. Ajdari, Appl. Phys. Lett. **89**, 034104 (2006).
[17]W. Engl, M. Roche, A. Colin, P. Panizza, and A. Ajdari, Phys. Rev. Lett. **95**, 208304 (2005).
[18]D. A. Sessoms, M. Belloul, W. Engl, M. Roche, L. Courbin, and P. Panizza, Phys. Rev. E **80**, 016317 (2009).
[19]D. Link, E. Grasland-Mongrain, A. Duri, F. Sarrazin, Z. Cheng, G. Cristobal, M. Marquez, and D. Weitz, Angew. Chem., Int. Ed. **45**, 2556 (2006).
[20]T. H. Ting, Y. F. Yap, N. T. Nguyen, T. N. Wong, J. C. K. Chai, and L. Yobas, Appl. Phys. Lett. **89**, 234101 (2006).
[21]X. Niu, M. Zhang, J. Wu, W. Wen, and P. Sheng, Soft Matter **5**, 576 (2009).
[22]C. N. Baroud, M. R. de Saint Vincent, and J.-P. Delville, Lab Chip **7**, 1029 (2007).
[23]K. Zhang, Q. Liang, X. Ai, P. Hu, Y. Wang, and G. Luo, Lab Chip **11**, 1271 (2011).
[24]Y. C. Tan, J. S. Fisher, A. I. Lee, V. Cristini, and A. P. Lee, Lab Chip **4**, 292 (2004).
[25]M. Prakash and N. Gershenfeld, Science **315**, 832 (2007).
[26]L. F. Cheow, L. Yobas, and D. L. Kwong, Appl. Phys. Lett. **90**, 054107 (2007).
[27]M. A. Cartas-Ayala, M. Raafat, and R. Karnik, Small **9**, 375 (2013).
[28]T. Cubaud and C. Ho, Phys. Fluids **16**, 4575 (2004).
[29]P. Parthiban and S. A. Khan, Lab Chip **12**, 582 (2012).
[30]M. Schindler and A. Ajdari, Phys. Rev. Lett. **100**, 044501 (2008).
[31]C. N. Baroud, F. Gallaire, and R. Dangla, Lab Chip **10**, 2032 (2010).
[32]M. J. Fuerstman, A. Lai, M. E. Thurlow, S. S. Shevkoplyas, H. A. Stone, and G. M. Whitesides, Lab Chip **7**, 1479 (2007).
[33]H. Bruus, *Theoretical Microfluidics* (Cambridge University Press, 1982), p. 51.
[34]See supplementary material at http://dx.doi.org/10.1063/1.4819276 for additional plots of experimental measurements, details regarding analytical derivation, and schematics of experimental setups.
[35]J. Jovanovic, W. Zhou, E. V. Rebrov, T. A. Nijhuis, V. Hessel, and J. C. Schouten, Chem. Eng. Sci. **66**, 42 (2011).
[36]F. Bretherton, J. Fluid Mech. **10**, 166 (1961).
[37]H. Wong, C. J. Radke, and S. Morris, J. Fluid Mech. **292**, 95 (1995).
[38]M. Kreutzer, F. Kapteijn, J. Moulijn, C. Kleijn, and J. Heiszwolf, AIChE J. **51**, 2428 (2005).
[39]B. J. Adzima and S. S. Velankar, J. Micromech. Microeng. **16**, 1504 (2006).
[40]S. A. Vanapalli, A. G. Banpurkar, D. van den Ende, M. H. G. Duits, and F. Mugele, Lab Chip **9**, 982 (2009).
[41]S. R. Hodges, O. E. Jensen, and J. M. Rallison, J. Fluid Mech. **501**, 279 (2004).
[42]M. Yamada, S. Doi, H. Maenaka, M. Yasuda, and M. Seki, J. Colloid Interface Sci. **321**, 401 (2008).
[43]J. Ratulowski and H. C. Chang, J. Fluid Mech. **210**, 303 (1990).
[44]J. L. Anderson, D. W. Armstrong, and G.-T. Wei, Anal. Chem. **78**, 2892 (2006).